Research Article

PHOTOCATALYTIC DEGRADATION OF METRONIDAZOLE USING BIOI–MWCNT COMPOSITES: SYNTHESIS, CHARACTERIZATION, AND OPERATIONAL PARAMETERS

**Davoud BALARAK[1], Chinenye Adaobi IGWEGBE*[2],
Pius Chukwukelue ONYECHI[3]**

[1]*Department of Environmental Health, Health Promotion Research Center, School of Public Health, Zahedan
University of Medical Sciences, Zahedan, IRAN;* ORCID: 0000-0003-3679-9726
[2]*Department of Chemical Engineering, Nnamdi Azikiwe University, Awka-NIGERIA;*
ORCID: 0000-0002-5766-7047
[3]*Department of Industrial/Production Engineering, Nnamdi Azikiwe University, Awka-NIGERIA;*
ORCID: 0000-0002-9612-4272

ABSTRACT

This study centers on the application of photocatalytic process using supported bismuth (III) oxyiodide–multi-walled carbon nanotube (BiOI–MWCNT) composites for the elimination of Metronidazole (MNZ) from its solution. The characteristics of BiOI and synthesized BiOI–MWCNTs composites were analyzed via the scanning electronic microscopy (SEM), X-ray diffraction (XRD), and transmission electron microscopy (TEM). The photocatalytic study was performed to evaluate the effect of UV (8, 15, 30, and 125 W), irradiation time (10–90 min), pH (5-9), initial MNZ concentration (10-100 mg/L) and BiOI–MWCNTs dosage (0.3–1.2 g/L) on MNZ removal at fixed neutral pH of 7. MNZ concentration was examined via the HPLC by measuring at 348 nm. Higher MNZ degradation was achieved using both BiOI–MWCNTs and UV light than using each separately. Maximum MNZ degradation efficiency of 99.95 % was obtained at pH 7, BiOI–MWCNTs dosage of 0.6g/L, MNZ concentration of 10mg/L, and irradiation time of 90min. MNZ removal was increased by increasing irradiation time and decreasing initial MNZ concentration. Pseudo-first-order rate of reaction (K) based on the Langmuir-Hinshelwood (L-H) model and adsorption equilibrium constant of 1.629 mg/L.min and 0.044 L/mg, respectively were obtained. Also, the adsorption kinetic study fitted the pseudo-first-order reaction. The electrical energy consumption per order of magnitude (E) for MNZ degradation was lower for the UV/BiOI–MWCNTs process than the BiOI–MWCNTs- alone and UV- alone processes. The photocatalytic degradation process using BiOI–MWCNTs can be applied efficiently for the removal of MNZ from aqueous solutions.
Keywords: Metronidazole, BiOI–MWCNTs, nanocomposites, photocatalytic oxidation, Langmuir-Hinshelwood model.

---

* Corresponding Author: e-mail: ca.igwegbe@unizik.edu.ng, tel: +2348036805440

1. INTRODUCTION

Recently, different kinds of evolving pollutants in water are identified as new hazards that are required to be removed through appropriate techniques [1, 2]. Since several pharmaceutical compounds have been applied owing to the expansion of medical science and speedy growth in the world's population and, numerous pharmaceutical materials have been observed in groundwater and surface water, and wastes from wastewater treatment plants [3, 4]. In developed countries, most humans use anti-microbials and other pharmaceuticals that reach the aquatic habitat, unchanged or altered, mainly through the release of effluents from municipal wastewater treatment plants [5, 6]. Antibiotics concentration less than 1 mg/L in effluents was set by the department of environmental standards, USA [7, 8]. Metronidazole (MNZ), a nitroimidazole anti-infective prescription is very active for the management of intraabdominal and intestinal infections. The toxic effects of MNZ in low concentrations against daphnids and algae have been stated recently [9, 10]. The concentrations of metronidazole in surface waters and wastewater are 1~10 ng/L [11]. Since MNZ is highly soluble in water and non-biodegradable, it can accumulate in the aquatic environs [12].

Many methods have been applied to eliminate antibiotics, such as Fenton and photo-Fenton processes, electro-Fenton process, adsorption, biological methods, ozonation technology, photolysis, and photocatalysis [8, 10-18]. Treatment processes such as sedimentation, coagulation-flocculation, and filtration are the most widely used methods in conventional wastewater treatment plants, but they have the disadvantage of not degrading contaminants that concentrate in the solid phase which creates a new source of pollution [19-21]. Adsorption is the most extensively applied procedure for the treatment of water and wastewater containing toxic organic compounds [22-24]. Also, adsorption only transfers pollutants from water to a solid phase without any degradation [25].

Due to the aforementioned setbacks, a valid alternative approach is to utilize advanced oxidation processes (AOPs) [26, 27]. These processes are based on the generation of intermediate radicals as hydroxyl radicals ($\cdot$OH), which are less selective than other oxidants and highly reactive because their standard oxidation potential is greater than the conventional oxidants [28-30]. Sometimes, the creation of the metabolites is more hazardous than the parent compound [31, 32].

Recently, research for highly efficient photocatalysts with a narrow bandgap that functions in the visible light region has drawn significant attention [33]. Favorable results have been attained using BiOI with the narrow bandgap in the application of the photocatalytic degradation for organic compounds [34]. In recent times, carbon nanotubes (CNTs)-coupled composites have been established to be very effective in enhancing the charge transfer between the interfaces of the nanostructure and display high catalytic action, owing to the outstanding charge transfer features and hollow geometry of CNTs [35, 36]. Considering that the CNTs possess large specific surface areas and outstanding charge transfer properties, thus, MWCNT-doped BiOI would be expected as a high efficient system with the apparent synergetic effect of adsorption and degradation for the organic contaminants owing to enhancement in charge separation via photoinduced electron transfer by MWCNTs [37].
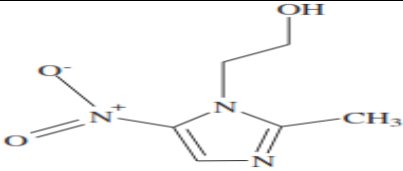
Therefore, in the present work, MWCNT-doped BiOI was selected as the catalyst in the photocatalytic removal of MNZ. The effects of working parameters including MWCNTs-doped BiOI dosage and initial MNZ concentration on the photocatalytic degradation of MNZ were investigated. The photocatalytic degradation kinetic parameters were evaluated via the Langmuir–Hinshelwood (L–H) model. Finally, the electrical energy per order (E) was determined to estimate the cost-efficiency of the processes used in this research.

2. MATERIALS AND METHODS

2.1. Chemicals and Reagents

Metronidazole ($C_6H_9N_3O$; 99% purity) of analytical grade was procured from Merck (Darmesdat, Germany). Table 1 presents its physical and chemical characteristics. Bismuth (iii) nitrate (Bi $(NO_3)_3 \cdot 5H_2O$, 98% purity), potassium iodide (KI, 99.9% purity), sodium hydroxide (NaOH, 99% purity), and hydrogen chloride (HCl, 99% purity) of analytical grade were obtained from Merck Co. (Germany). The multi-wall carbon nanotubes (MWCNTs, 98% purity) used in this study were acquired from the Research Institute of Petroleum Industry (RIPI), Tehran, Iran. Double-distilled water was used to prepare all solutions.

Table 1. Properties of metronidazole (MNZ).

Characteristic	Metronidazole antibiotic (MNZ)
Molecular structure	
Molecular formula	$C_6H_9N_3O$
Molecular weight (g/mol)	171.2
Water solubility (g/L)	9.5
Melting point (°C)	59-163
pKa	2.55

2.2. Preparation of the BiOI–MWCNTs Composites

BiOI was prepared using the ethylene glycol (EG)-assisted solvothermal method based on a previous account [33]. Firstly, potassium iodide (KI) and bismuth (III) nitrate (Bi $(NO_3)_3 \cdot 5H_2O$) of equal molar ratio (1:1) were added into an ethylene glycol solution. The mixture was agitated for 30 min using a magnetic shaker. Then, the mixture was sonicated for 30 min to form a homogeneous phase. The sonicated mixture was then autoclaved at 160 °C for 12 h until 80 % of the volume was filled. Finally, the precipitate was centrifuged, filtered through a 0.22 µm membrane, and washed thrice with ethanol and double-distilled water. In order to prepare the BiOI–MWCNTs composites, the MWCNTs were washed with a 0.1 M NaOH solution and double-distilled water. The washed MWCNTs sample was dried at 75 ^{0}C for 6 h. Then, 1.0% of the purified MWCNTs were added into the previously mixed salts of potassium iodide and bismuth (III) nitrate.

2.3. Batch experimental procedure

All photocatalytic degradation experiments were done in batch mode in a photoreactor with a working volume of 1 L. A UV lamp which is placed inside the photoreactor was operated as the radiation source. The light intensity on the surface of the solution was UV-C, 11.2 W/m^2. The light intensity was determined by the CASSY Lab (Germany). The MNZ solution was prepared by dissolving a known mass of MNZ in 1000 mL of double-distilled water. For the experiments, a certain dose of BiOI- MWCNTs (0.25-2 g/L) was put into 1000 mL of MNZ solution with a definite concentration (25–100 mg/L) at fixed pH of 7. The pH of the MNZ solution was attuned by adding 0.1 mol/L NaOH and HCl. The pH of the samples was measured with a pH meter

(Metron, Switzerland). The MNZ solution with the catalyst in the photoreactor was stirred constantly with a magnetic stirrer at 170 rpm at a constant temperature of $25 \pm 2°C$ for 90 min. The mixture was then equilibrated in the shade for 30 min and the UV-lamp was turned on. 10 mL of the solution was collected at different times. Then, the samples were centrifuged at speed of 4000 rpm for 10 min to get rid of the BiOI-MWCNTs and then the residual MNZ concentration was measured.

The residual MNZ concentration was determined as described by Farzadkia et al. [12]. The MNZ degradation efficiency ($\%R_{MNZ}$) was evaluated using Eq. (1) [38]:

$$\%R_{MNZ} = \frac{C_0 - C_f}{C_0} \times 100 \tag{1}$$

where C_0 and C_f are the initial and residual MNZ concentrations (mg/L), respectively.

3. RESULTS AND DISCUSSION

3.1. Characterization of the BiOI and BiOI–MWCNT composites

Scanning electron microscopy (SEM) was employed to reveal the morphology of BiOI and BiOI–MWCNT composites. The SEM images of BiOI and BiOI–MWCNT composites are displayed in Figure 1. Both BiOI and BiOI–MWCNTs are microspheres with porous surfaces. The BiOI-MWCNT composites' surface (Figure 1b) was less porous than the BiOI surface (Figure 1a), showing that the MWCNTs played a great role in the development of crystals [34].

Figure 2 shows the TEM pictures of BiOI–MWCNTs and BiOI. The BiOI comprised of well-structured spheres (Figure 2b). Irregular nanoplates were also observed on the surface of BiOI microspheres. The MWCNTs were well intertwined among the BiOI (Figure 2b); this can accelerate the charge transfer from the exited BiOI to MWCNTs which will result in increased photocatalytic performance [33].

The XRD patterns of the BiOI–MWCNTs (Figure 3) showed that all peaks of the BiOI sample are without any characteristic peaks of other impurities, which indicated that well-crystallized BiOI can be prepared by the EG-assisted solvothermal method. The peak of MWCNTs at 27.2 is seen in accompany with XRD patterns of BiOI, showing that the BiOI–MWCNTs composites with the coexistence of BiOI and MWCNTs phase were synthesized.
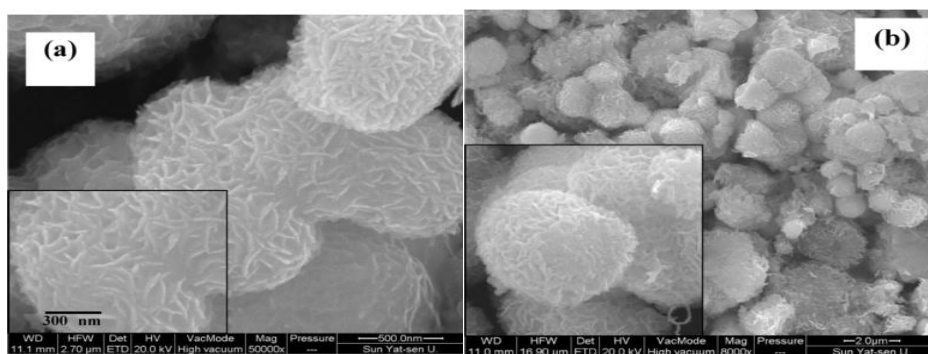

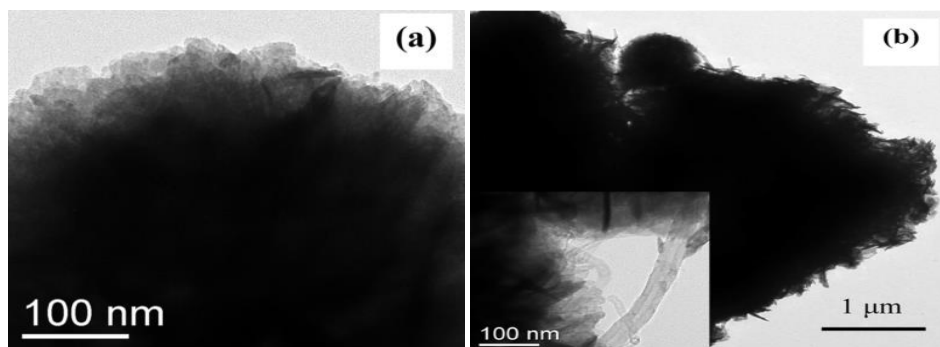**Figure 1.** SEM images of (a) BiOI and (b) BiOI–MWCNTs

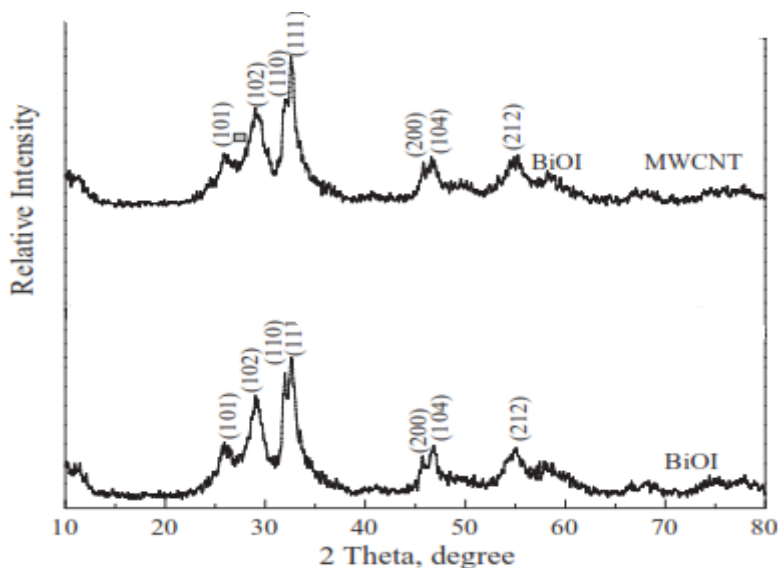**Figure 2.** TEM images of (a) BiOI and (b) BiOI–MWCNTs

Figure 3. XRD patterns of BiOI–MWCNT composites.

3.2. Effect of BiOI–MWCNTs dosage

The effect of BiOI–MWCNTs dosage (0.3–1.2 g/L) on the photocatalytic degradation of MNZ was examined at a pH of 7 using MNZ concentration of 10 mg/L and UV of 125 W. As shown in Figure 4, the degradation efficiency was increased as the dosage of BiOI–MWCNTs was increased from 0.3 to 0.6 g/L but decreased further when the dosage was increased from 0.6 to 1.2 g/L at all irradiation times. Also, the degradation of MNZ was improved from 56.93 to 99.95 % by increasing the irradiation time from 10 to 90 min at the optimum BiOI–MWCNTs dosage of 0.6 g/L. Higher degradation was noticed over the entire irradiation time at a low dosage. This may be due to the increased blockage of the incident UV light with increasing BiOI–MWCNTs dosage [39]. Similar observations have been noted by other authors [40, 41].
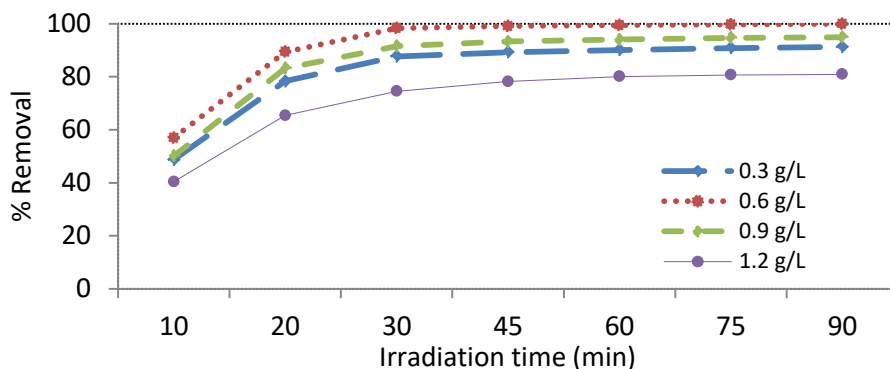
Figure 4. Effect of BiOI–MWCNTs dosage on photocatalytic degradation of MNZ (C0 = 10 mg/L, pH=7, UV=125 W)

3.3. Effect of UV radiation and UV/BiOI–MWCNTs

The effect of UV radiation (8, 15, 30, and 125 W) alone on MNZ degradation was studied at a pH of 7 using MNZ concentration (C_0) of 10 mg/L. Their degradation efficiency was compared with using BiOI–MWCNTs alone. Figure 5 shows the removal of MNZ using BiOI–MWCNTs-alone, UV 8 W-alone, UV 15 W-alone, UV 30 W-alone and UV 125 W alone. The removal of MNZ using all was low throughout the adsorption process even at different times. The removal efficiencies of MNZ by BiOI–MWCNTs-alone, UV 8 W-alone, UV 15 W-alone, UV 30 W-alone and UV 125 W-alone were 61.59, 29.84, 38.61, 47.72, and 58.53 %, respectively. From these values, it can also be seen that the degradation efficiency was increased as the UV intensity was increased from 8 to 125 W. Therefore, 125 W is the optimal UV intensity. Also, using BiOI–MWCNTs-alone gave the best performance than using UV-alone (Figure 5) since BiOI–MWCNTs is a catalyst.

But 83.25, 90.14, 96.04 and 99.95% of MNZ were removed with the combinations, UV 8 W/BiOI–MWCNTs, UV 15 W/BiOI–MWCNTs, UV 30 W/BiOI–MWCNTs and UV 125 W/BiOI–MWCNTs, respectively at pH of 7 using MNZ concentration of 10 mg/L and BiOI–MWCNTs dosage of 0.6 g/L (Figure 6). This study established that both BiOI–MWCNTs and UV light are essential for the effective removal of MNZ. Similar reports have been made by other researchers [42, 43].
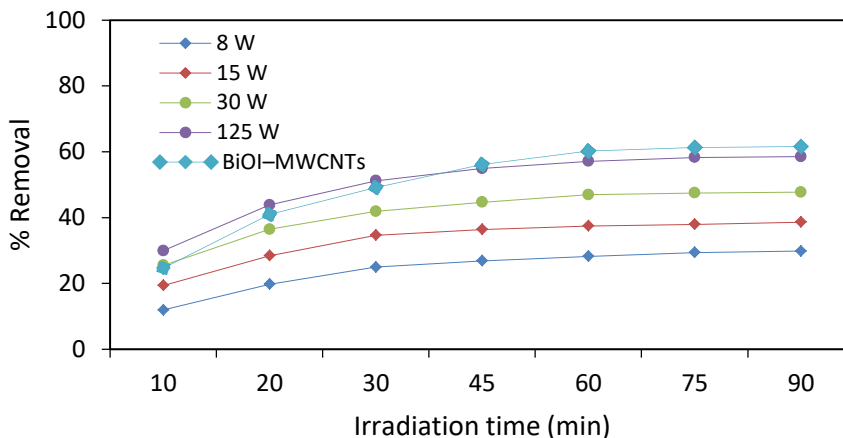
Figure 5. Effect of UV light on the photocatalytic reduction of MNZ (C0 = 10 mg/L, pH=7)

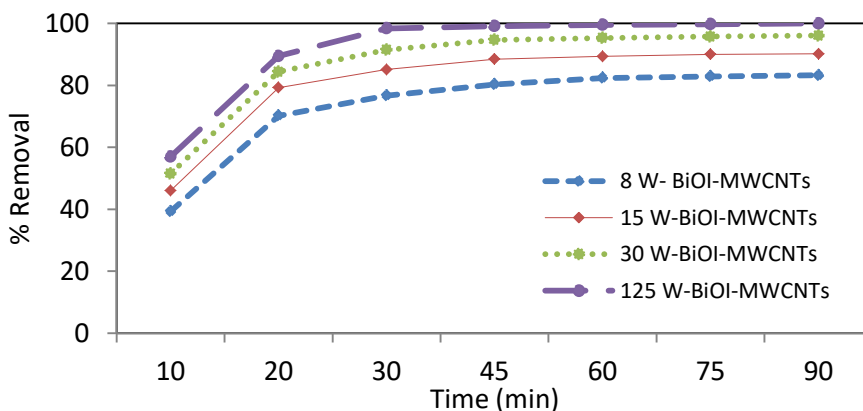**Figure 6.** Effect of BiOI–MWCNTs and UV light on photocatalytic reduction of MNZ (C0= 10 mg/L, pH=7, BiOI–MWCNTs dosage = 0.6 g/L).

3.4. Effect of initial MNZ concentration

The influence of initial MNZ concentration on the degradation of MNZ by BiOI–MWCNTs was examined by changing the initial MNZ concentration from 10 to 100 mg/L at pH 7 using BiOI–MWCNTs dosage of 0.6 g/L and UV of 125 W. Figure 7 displays that the degradation efficiency declined with increasing MNZ concentration from 10 to 100 mg/L at different times. The presumed reason is that more surface of the BiOI–MWCNTs may be occupied by MNZ, as the initial MNZ concentration increased [44, 45].

Also, more degradation intermediates can be collected on the surface of the BiOI–MWCNTs resulting in a negative effect on the hydroxyl radicals or positive holes in the valence band of the BiOI–MWCNTs [12, 46]. Moreover, as the concentration of the MNZ increases, there will be more absorption of UV light by the molecules of MNZ, which is known as the inner filtration effect, can occur [47]. This effect results in a decrease of photons getting to the BiOI–MWCNTs surface. Similar results have been stated by other researchers [48].
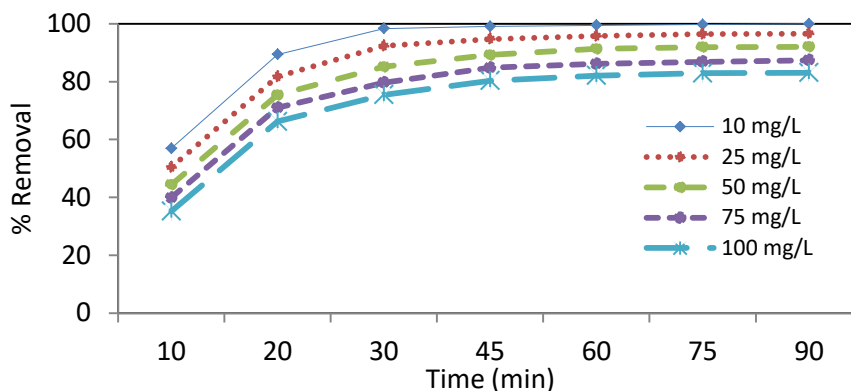
Figure 7. Effect of MNZ concentration on the photocatalytic degradation of MNZ (pH=7, BiOI–MWCNTs dosage = 0.6 g/L and UV=125 W)

3.5. Kinetics of Photocatalytic Degradation of MNZ

The data of the photocatalytic degradation of MNZ using BiOI–MWCNTs were fitted into the pseudo-first-order rate equation at different initial MNZ concentrations. The pseudo-first-order rate equation is given by Eq. (2) [49, 50]:

$$Ln\left[\frac{C_0}{C_t}\right] = Kt \tag{2}$$

Where K is the pseudo-first-order rate constant, C_0 and C_t are the concentration at time t and $t = 0$, respectively.

The pseudo-first-order rate constants were obtained from the slopes of the linear plots of Ln (C_0/C_t) versus t (Figure 8). The values of the pseudo-first-order rate constants (K) at different initial concentrations are presented in Table 2. The pseudo-first-order rate constants obtained for the photocatalytic degradation of MNZ decreased as the initial MNZ concentration was increased. This may be attributed to the reduction in the number of active sites on the photocatalyst surface as a result of the blocking of the BiOI–MWCNTs surface with MNZ molecules, which is directly proportional to the initial MNZ concentration [51, 52]. The values of the regression coefficients (R^2) indicate that the photocatalytic removal of MNZ using BiOI–MWCNTs followed the pseudo-first-order rate reaction (Table 2).
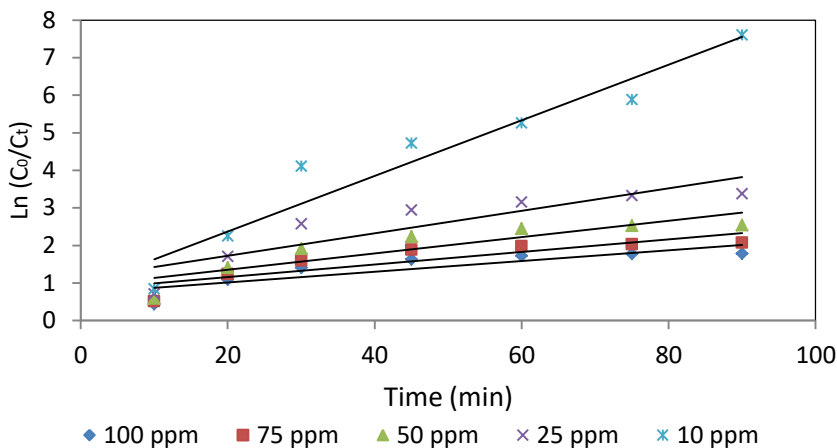
Figure 8. First-order kinetic model plot for the photocatalytic degradation of MNZ (BiOI–MWCNTs dosage = 0.6 g/L, pH = 7).

Table 2. Pseudo-first-order kinetic rate constants at different initial concentrations.

C_0 (mg/L)	K (1/min)	R^2
10	0.074	0.928
25	0.029	0.936
50	0.021	0.945
75	0.016	0.951
100	0.014	0.941

Many authors have successfully applied the modified Langmuir Hinshelwood (L-H) kinetic equation to study the photocatalytic reaction [53]. The oxidation rate at the surface reaction is directly proportional to the surface covered by MNZ on the BiOI–MWCNTs while assuming that the MNZ is strongly adsorbed on the BiOI–MWCNTs surface than the intermediate products [54]. The relationship between the rate of initial photocatalytic degradation (r) and the initial concentration of organic substrate for a heterogeneous photocatalytic process can be described by the Langmuir–Hinshelwood (L-H) model equation (Eqs. (3)) [55, 56].

$$r = \frac{K_C K_{MNZ}(C)}{1 + K_{MNZ}(C_0)} = KC \tag{3}$$

Linearizing Eq. (3), Eq. (4) is obtained as:

$$\frac{1}{K} = \frac{1}{K_C K_{MNZ}} + \frac{(C_0)}{K_C} \tag{4}$$

Where C_0 is the initial concentration of the MNZ in mg/L, K_{MNZ} the Langmuir-Hinshelwood adsorption equilibrium constant and K_c is the rate constant of surface reaction, respectively. The K_{MNZ} and K_c values were estimated as 0.044 L/mg and 1.629 mg/L/min, respectively from the slope and intercept of the straight-line plots of $1/K$ versus C_0, respectively using Eq. (4). The value of the regression coefficient, R^2 (0.9523) indicates that the photocatalytic removal of MNZ using BiOI–MWCNTs followed the Langmuir-Hinshelwood model (Figure 9).
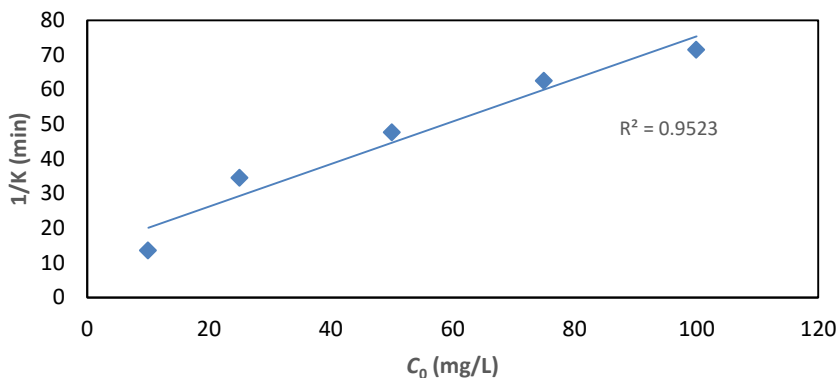
Figure 9. Langmuir-Hinshelwood plot for the photocatalytic degradation of MNZ (BiOI–MWCNTs dosage = 0.6 g/L, pH = 7).

3.6. Electrical energy determination

The electrical energy per order (E) is defined as the number of kWh of electrical energy required to reduce the concentration of a pollutant by 1 order of magnitude (90%) in 1 m^3 of contaminated water [12]. Electrical energy per order (E) was determined in this study since it is a very significant factor for photocatalytic reactions. The E (KWh/m^3) was evaluated using Eq. (5) [57, 58]:

$$E = \frac{1000Pt}{60V \text{ Log}(\frac{C_0}{C_t})} \tag{5}$$

Where P is the lamp power (kW), t is the irradiation time (min), and V is the volume of the wastewater in the reactor (L); C_0 and C_t are the initial and final MNZ concentrations, respectively. The E values using different intensities of UV-alone and different combinations of UV/BiOI–MWCNTs are reported in Table 3. As seen in Table 3, the E values for UV/BiOI–MWCNTs process was lower than the UV-alone process. This implies that less electrical energy is required when BiOI–MWCNTs catalyst is added to the degradation process.

Table 3. The electrical energy per order values for the degradation of MNZ (at C_0 = 10 mg/L, BiOI–MWCNTs dosage = 0.6 g/L and pH = 7).

Process	E (KWh/m^3)	Process	E (KWh/m^3)
UV 8 W-alone	77.96	UV 8 W/BiOI–MWCNTs	15.46
UV 15 W-alone	106.1	UV 15 W/BiOI–MWCNTs	22.36
UV 30 W-alone	159.7	UV 30 W/BiOI–MWCNTs	32.09
UV 125 W-alone	490.4	UV 125 W/BiOI–MWCNTs	56.8

3.7. Removal of MNZ using other photocatalysts

The removal of metronidazole (MNZ) using BiOI–MWCNT composite was compared with other photocatalysts used by different authors (Table 2). From Table 4, it can be seen that the BiOI–MWCNTs were effective during the photodegradation of MNZ compared with the other photocatalysts. It was also observed the UV/BiOI–MWCNTs gave the best performance on MNZ degradation with an efficiency of 99.95%. The results obtained by the authors (Table 4) and this

study also proved that the photocatalytic degradation process of water treatment is a capable technique for MNZ reduction.

Table 4. Comparison of BiOI–MWCNT composites with other photocatalysts for metronidazole reduction.

Photocatalysts	Mechanism	Maximum removal (%)	K (min^{-1})	Conditions	Reference
Titanium (IV) oxide nanoparticles (TiO$_2$)	UV/TiO$_2$	99.48	0.0233	pH = 7; Dosage of catalyst = 0.5 g/L; Initial concentration=80 mg/L; Lamp = 15 W; Time = 120 min; Volume of MNZ solution, V =100 mL; Temperature = 25 ± 1°C; Speed = 170 rpm	[12]
Copper (II) oxide nanoparticles CuO	UV/CuO	97.0	0.0198	pH = 2; Dosage of catalyst = 0.1 g/L; Initial MNZ concentration = 25 mg/L; Lamp = 125 W; Time = 120 min; V = 1000 mL	[59]
Zero valent-iron nanoparticles (nZVI)	Nano/Persulfate (nZVI/PS)	90.3	-	pH = 3; Dosage of catalyst = 0.5 g/L; Initial MNZ concentration = 1 mg/L; Time = 30 min; PS concentration = 1.85 mM	[60]
Bismuth (III) oxyiodide–multi-walled carbon nanotube (BiOI–MWCNT) composites	UV/BiOI–MWCNTs	99.95	0.0740	pH = 7; Dosage of catalyst = 0.6 g/L; Initial MNZ concentration = 10 mg/L; Lamp = 30 W; Time = 90 min; V = 1000 mL; Temperature = 25 ± 2°C; Speed = 170 rpm	This study

4. CONCLUSIONS

Bismuth (III) oxyiodide–multi-walled carbon nanotube (BiOI–MWCNT) composites were applied as a catalyst for the photocatalytic elimination of Metronidazole (MNZ) from its solution. The results indicated that the extent of photocatalytic degradation of MNZ was evidently influenced by illumination time, initial MNZ concentration, BiOI–MWCNTs dosage, and UV intensity. Higher MNZ degradation was achieved using both BiOI–MWCNTs and UV light than using each separately. The photocatalytic reduction of MNZ fitted into the Langmuir-Hinshelwood model. The electrical energy consumption per order of magnitude (E) for photocatalytic degradation of MNZ was lower for the UV/ BiOI–MWCNTs process than the UV- and BiOI–MWCNTs- alone processes. The photocatalytic degradation process using BiOI–MWCNTs can be applied efficiently for the removal of MNZ from aqueous solutions.

Acknowledgement

REFERENCES

[1]   Balarak D., Azarpira H., (2016) Photocatalytic degradation of Sulfamethoxazole in water: investigation of the effect of operational parameters, *International J. ChemTech Res.* 9, 731-8.

[2]   Ahmadi S., Banach A., Kord Mostafapour F., (2017) Study survey of cupric oxide nanoparticles in removal efficiency of ciprofloxacin antibiotic from aqueous solution: Adsorption isotherm study, *Desal. Water Treat.* 89, 297-303.

[3]   Balarak D., Azarpira H., Mostafapour F.K., (2016) Study of the Adsorption Mechanisms of Cephalexin on to *Azolla Filiculoides*, *Der Pharma Chemica* 8, 114-121.

[4]   Liu Z., Xie H., Zhang J., Zhang C., (2012) Sorption removal of cephalexin by HNO_3 and H_2O_2 oxidized activated carbons, *Sci. China Chem.* 55, 1959–67.

[5]   Liu H., Liu W., Zhang J., Zhang C., Ren L., Li Y., (2011) Removal of cephalexin from aqueous solution by original and Cu (II)/Fe (III) impregnated activated carbons developed from lotus stalks kinetics and equilibrium studies, *J. Hazard Mater.* 185, 1528–35.

[6]   Yu F., Li Y., Han S., Jie Ma J., (2016) Adsorptive removal of antibiotics from aqueous solution using carbon Materials, *Chemosphere* 153, 365–385.

[7]   Mohammadi A.S., Yazdanbakhsh A.R., Sardar M., (2013) Chemical oxygen demand removal from synthetic wastewater containing non-beta lactam antibiotics using advanced oxidation processes: A comparative study, *Arch. Hyg. Sci.* 2, 23-30.

[8]   Rahdar S., Rahdar A., Igwegbe C.A., Moghaddam F., Ahmadi S., (2019) Synthesis and physical characterization of nickel oxide nanoparticles and its application study in the removal of ciprofloxacin from contaminated water by adsorption: Equilibrium and kinetic studies, *Desal. Water Treat.* 141, 386–393.

[9]   Balarak D., Azarpira H., (2016) Rice husk as a biosorbent for antibiotic metronidazole removal: isotherm studies and model validation, *International Journal of ChemTech Research* 9, 566-573.

[10]   Azarpira H., Mahdavi Y., Khaleghi O., (2016) Thermodynamic studies on the removal of metronidazole antibiotic by multi-walled carbon nanotubes, *Der Pharmacia Lettre* 8, 107-13.

[11]   Shemer H., Kunukcu Y.K., Linden K.G., (2006) Degradation of the pharmaceutical Metronidazole via UV, Fenton and photo-Fenton processes, *Chemosphere* 63, 269-276.

[12]   Farzadkia M., Esrafili A., Yang J.K., Siboni M.S., (2015) Photocatalytic degradation of Metronidazole with illuminated TiO_2 nanoparticles, *Journal of Environmental Health Science and Engineering* 13, 35-44.

[13]   Zhang W., He G., Gao P., Chen G., (2003) Development and characterization of composite nanofiltration membranes and their application in concentration of antibiotic, *Sep. Purif. Technol.* 30, 27–35.

[14]   Gao J., Pedersen J.A., (2005) Adsorption of sulfonamide antimicrobial agents to clay minerals, *Environ. Sci. Technol.* 39, 9509-16.

[15]   Peterson J.W., Petrasky L.J., Seymourc M.D., Burkharta R.S., Schuilinga A.B., (2012) Adsorption and breakdown of penicillin antibiotic in the presence of titanium oxide nanoparticles in water, *Chemosphere* 87, 911–7.

[16]   Rahdar S., Igwegbe C.A., Rahdar A., Ahmadi S., (2018) Efficiency of sono-nano-catalytic process of magnesium oxide nanoparticle in removal of penicillin G from aqueous solution, *Desalin. Wat. Treat.* 106, 330–335.

[17]   Homem V., Santos L., (2011) Degradation and removal methods of antibiotics from aqueous matrices-A review, *J. Environ. Manage.* 92, 2304-2347.

[18]   Yoosefian M., Ahmadzadeh S., Aghasi M., Dolatabadi M., (2017) Optimization of electrocoagulation process for efficient removal of ciprofloxacin antibiotic using iron electrode; kinetic and isotherm studies of adsorption, *J. Mole. Liq.* 225, 544-553.

[19]   Ghauch A., Tuqan A., Abou A.H., (2009) Antibiotic removal from water: Elimination of amoxicillin and ampicillin by microscale and nanoscale iron particles. Environ Pollut. 157, 1626–1635.

[20]   Alexy R., Kumpel T., Kummerer K., (2004) Assessment of degradation of 18 antibiotics in the closed bottle test, *Chemosphere* 57, 505–512.

[21]   Carabineiro A., Thavorn-Amornsri T., Pereira F., Figueiredo L., (2011) Adsorption of ciprofloxacin on surface modified carbon materials, *Water Res.* 45, 4583-91.

[22]   Peng X., Hu F., Dai H., Xiong Q., (2016) Study of the adsorption mechanism of ciprofloxacin antibiotics onto graphitic ordered mesoporous carbons, *Journal of the Taiwan Institute of Chemical Engineers* 8, 1–10.

[23]   Balarak D., Azarpira H., Mostafapour F.K., (2016) Adsorption isotherm studies of tetracycline antibiotics from aqueous solutions by maize stalks as a cheap biosorbent, *International Journal of Pharmacy & Technology* 8, 16664-75.

[24]   Mahvi A.H., Mostafapour F.K., (2018) Biosorption of tetracycline from aqueous solution by *Azolla filiculoides*: equilibrium, kinetic and thermodynamics studies, *Fresenius Environmental Bulletin* 27, 5759-5767.

[25]   Balarak D., Mostafapour F., Bazrafshan E., Saleh T.A., (2017) Studies on the adsorption of amoxicillin on multi-wall carbon nanotubes, *Water Science and Technology* 75, 1599-1606.

[26]   An T., Yang H., Li G., Song W., Nie X., (2010) Kinetics and mechanism of advanced oxidation processes (AOPs) in degradation of ciprofloxacin in water, *Applied Catalysis B: Environmental* 94, 288–94.

[27]   Fairooz N.Y., (2016) Evaluation of new couple Nb_2O_5/Sb_2O_3 oxide for photocatalytic degradation of Orange G dye, *International Journal of ChemTech Research* 9, 456-61.

[28]   Hayat K., Gondal M.A., Khaled M.M., Ahmed S., Shemsi A.M., (2011) Nano ZnO synthesis by modified sol gel method and its application in heterogeneous photocatalytic removal of phenol from water, *Applied Catalysis A: General* 393, 122–29.

[29]   Fan J., Hu X., Xie Z., Zhang K., Wang J., (2012) Photocatalytic degradation of azo dye by novel Bi-based photocatalyst Bi4TaO8I under visible-light irradiation, *Chem. Eng. J.* 179, 44–51.

[30]   Ahmadi S., Igwegbe C.A., Rahdar S., (2009) The application of thermally activated persulfate for degradation of Acid Blue 92 in aqueous solution, *Int. J. Ind. Chem.*

[31]   Asahi R., Morikawa T., Ohwaki T., Aoki K., Taga Y., (2011) Visible-light Photocatalysis in nitrogen-doped titanium oxides. Science 293, 269–71.

[32]   Karuppuchamy S., Kumar R. D., (2015) Synthesis and characterization of visible light active titanium dioxide nanomaterials for photocatalytic applications, *International Journal of ChemTech Research* 8, 287-83.

[33]   Su M., He C., Zhua L., Sun Z., Shan C., Zhang Q., (2012) Enhanced adsorption and photocatalytic activity of BiOI–MWCNT composites towards organic pollutants in aqueous solution, *J. Hazard. Mater.* 229–230, 72– 82.

[34]   Xia J., Yin S., Li H., Xu H., Yan Y., Zhang Q., (2010) Self-assembly and enhanced photocatalytic properties of BiOI hollow microspheres via a reactable ionic liquid, *Langmuir* 27, 1200-1206.

[35]   Tettey K.E., Yee M.Q., Lee D., (2010) Photocatalytic and conductive $MWCNT/TiO_2$ nanocomposite thin films, *ACS Appl. Mater. Interfaces* 2, 2646–2652.

[36]   Li S., Hu S., Xu K., Jiang W., Liu J., Wang Z., (2017) A novel heterostructure of BiOI nanosheets anchored onto MWCNTs with excellent visible-light photocatalytic activity, *Nanomaterials (Basel)* 7, 22.

[37]   Zhang X., Ai Z.H., Jia F.L., Zhang L.Z., (2008) Generalized one-pot synthesis, characterization, and photocatalytic activity of hierarchical BiOX nanoplate microspheres, *J. Phys. Chem., C* 112, 747–753.

[38]   Igwegbe C. A., Ahmadi S., Rahdar S., Ramazani A., Mollazehi A.R., (2020) Efficiency comparison of advanced oxidation processes for ciprofloxacin removal from aqueous solutions: Sonochemical, sono-nano-chemical and sono-nano-chemical/persulfate processes, *Environ. Eng. Res.* 25(2), 178-185.

[39]   Guettai N., Amar H., (2005) Photocatalytic oxidation of methyl orange in presence of titanium dioxide in aqueous suspension. Part II. Kinetics study, *Desalination,* 185, 439-448.

[40]   Seidmohammadi G.A., Torabi L., (2016) Removal of metronidazole using ozone activated persulfate from aqua solutions in presence of ultrasound, *J. Mazandaran Univ. Med. Sci.* 26, 160-173.

[41]   Rivera-Utrilla J., Prados-Joya G., Sánchez- Polo M., Ferro-García M.A., Bautista-Toledo I., (2009) Removal of nitroimidazole antibiotics from aqueous solution by adsorption/bio-adsorption on activated carbon, *J. Hazard. Mater.* 170, 298-305.

[42]   Wang W.-L., Wu Q.-Y., Wang Z.-M., Hu H.-Y., Negishi N., Torimura M., (2015) Photocatalytic degradation of the antiviral drug Tamiflu by UV-A/TiO$_2$: Kinetics and mechanisms, *Chemosphere* 131, 41-47.

[43]   Pino N.J., Palominos R.A., Mansilla H.D., (2010) Degradation of the antibiotic oxolinic acid by photocatalysis with TiO$_2$ in suspension, *Water Res.* 44, 5158-5167.

[44]   Liu Y., Gan X., (2009) Photoelectrocatalytic degradation of tetracycline by highly effective TiO2 nanopore arrays electrode, *J. Hazard. Mater.* 171, 678-683.

[45]   Rodrigo A., Palominos A., (2009) Photocatalytic oxidation of the antibiotic tetracycline on TiO$_2$ and ZnO suspensions, *J. Catalysis Today* 114, 100–105.

[46]   Bu Q., Wang B., Huang J., Deng S., Yu G., (2013) Pharmaceuticals and personal care products in the aquatic environment in China: A review, *J. Hazard. Mater.* 262, 189-211.

[47]   Yang L., Yu L.E., Ray M.B., (2008) Degradation of paracetamol in aqueous solutions by TiO$_2$ photocatalysis, *Water Res.* 42, 3480-3488.

[48]   Xekoukoulotakis N.P., Xinidis N., Chroni M., Mantzavinos D., Venieri D., Hapeshi E., (2010) UV-A/TiO$_2$ photocatalytic decomposition of erythromycin in water: Factors affecting mineralization and antibiotic activity, *Catalysis Today* 151, 29-33.

[49]   Anandan S., Kathiravan K., Murugesan V., Ikuma Y., (2009) Anionic (IO$_3$) non-metal doped TiO$_2$ nanoparticles for the photocatalytic degradation of hazardous pollutant in water, *Catalysis Communications* 10, 1014–19.

[50]   Karthikeyan N., Narayanan V., Stephen A., (2015) Degradation of textile effluent using nanocomposite TiO$_2$/SnO$_2$ semiconductor photocatalysts, *International Journal of ChemTech Research* 8, 443-49.

[51]   Muruganaadham M., Swaminathan M., (2004) Solar photocatalytic degradation of a reactive azo dye in TiO$_2$-suspension, *Solar Energy Mater. Solar Cells* 81, 439–57.

[52]   Hequet V., Gonzalez C., Cloirec P.L., (2001) Photochemical processes for atrazine degradation: methodological approach, *Water Res.* 35, 4253–60.

[53]   Galindo C., Jacques P., Kalt A., (2000) Photodegradation of the aminoazobenzene acid orange 52 by three advanced oxidation processes: UV/H$_2$O$_2$, UV/TiO$_2$ and VIS/TiO$_2$, *Journal of Photochemistry and Photobiology A: Chemistry* 130, 35-47.

[54]   Vaiano V., Sacco O., Sannino D., Ciambelli P., (2014) Photocatalytic removal of spiramycin from wastewater under visible light with N-doped TiO$_2$ photocatalysts, *Chem. Eng. J.* 39, 42–50.

[55]   Behnajady M.A., Modirshahla N., Hamzavi R., (2006) Kinetic study on photocatalytic degradation of C.I. Acid yellow 23 by ZnO photocatalyst, *J. Hazard. Mater.,* 133, 226–232.

[56]   Bansal P., Singh D., Sud D., (2010) Photocatalytic degradation of azo dye in aqueous TiO$_2$ suspension: reaction pathway and identification of intermediates products by LC/MS, *Sep. Purif. Technol.* 72, 357–365.

[57] Chang X.F., Huang J., Tan Q.Y., Wang M., Ji G.B., Deng S.B., Yu G., (2009) Photocatalytic degradation of PCP-Na over BiOI nanosheets under simulated sunlight irradiation, *Catal. Commun.,* 10, 1957–1961.

[58] Balarak D., Mostafapour F.K., (2019) Photocatalytic degradation of amoxicillin using UV/Synthesized NiO from pharmaceutical wastewater, *Indonesian Journal of Chemistry* 19, 211-218.

[59] El-Sayed G.O., Dessouki H.A., Jahin H.S., Ibrahiem S.S., (2014) Photocatalytic degradation of metronidazole in aqueous solutions by copper oxide nanoparticles, *Journal of Basic and Environmental Sciences* 1, 102–110.

[60] Hamzehzadeh A., Fazlzadeh M., Rahmani K., (2017) Efficiency of nano/persulfate process (NZVI/PS) in removing metronidazole from aqueous solution, *J. Environ. Health Eng*. 4, 307-320.